MAPPING ALTERATION ZONES IN INACCESSIBLE REGIONS USING TARGET DETECTION ALGORITHMS TO SWIR BANDS OF ASTER REMOTE SENSING DATA

Amin Beiranvand Pour[1,2], Mazlan Hashim[1], Yongcheol Park[2] and Jong Kuk Hong[2]

[1]Geoscience and Digital Earth Centre (INSTeG),Universiti Teknologi Malaysia, 81310 UTM JB, Malaysia
Email: beiranvand.amin80@gmail.com; mazlanhashim@utm.my
[2]Korea Polar Research Institute (KOPRI), Songdomirae-ro,Yeonsu-gu, Incheon 21990, Republic of Korea
Email: ypark@kopri.re.kr; jkhong@kopri.re.kr

KEY WORDS: ASTER; SWIR; Geological mapping; Antarctic environments

ABSTRACT: In this study, the application of shortwave infrared (SWIR) bands of Advanced Spaceborne Thermal Emission and Reflection Radiometer (ASTER) data was investigated to extract geological information for alteration mineral mapping in inaccessible regions. The Oscar II coast area in the north-eastern Graham Land, Antarctic Peninsula (AP) was selected for this study to conduct a satellite-based remote sensing mapping technique. Target detection algorithms such as Constrained Energy Minimization (CEM), Orthogonal Subspace Projection (OSP) and Adaptive Coherence Estimator (ACE) were tested to ASTER shortwave infrared bands for detecting spectral features attributed to alteration mineral assemblages at district scale. Sub-pixels abundance of spectral features related to Al-O-H, Fe, Mg-O-H and CO3 mineral groups were detected using SWIR datasets of ASTER with little available geological data for poorly mapped regions and/or without prior geological information for unmapped regions in northern and southern sectors of Oscar II coast area, Graham Land. Fractional abundance of alteration minerals such as muscovite, kaolinite, illite, montmorillonite, epidote, chlorite and biotite were identified in alteration zones using CEM, OSP and ACE algorithms in poorly mapped and unmapped terrains at district scale. The results of this investigation demonstrated the applicability of SWIR bands of ASTER spectral data for alteration mineral mapping in inaccessible regions, particularly using the image processing algorithms that are capable to detect sub-pixel targets in the remotely sensed images, where no prior information is available.

1. INTRODUCTION

Remote sensing satellite imagery has high potential to provide a solution to overcome the difficulties and limitations associated with geological field mapping and mineral exploration in inaccessible regions (Pour et al., 2017 a,b). The Advanced Spaceborne Thermal Emission and Reflection Radiometer (ASTER) is a high spatial, spectral and radiometric resolution multispectral remote sensing sensor (Abrams et al., 2004). It consists of three separate instrument subsystems, which provide observation in three different spectral regions of the electromagnetic spectrum, including visible and near infrared (VNIR), shortwave infrared (SWIR) and thermal infrared (TIR). The VNIR subsystem has three recording channels between 0.52 and 0.86 µm with a spatial resolution of up to 15 m. The SWIR subsystem has six recording channels from 1.6 to 2.43 µm, at a spatial resolution of 30 m, while the TIR subsystem has five recording channels, covering the 8.125 to 11.65 µm wavelength region with spatial resolution of 90 m. ASTER swath width is 60km (each individual scene is cut to a 60x60 km^2 area) which makes it useful for regional geological mapping (Abrams et al., 2004).

There is plenty of research that used ASTER data in mineral exploration and lithological mapping during last decade due to spectral characteristics of the unique integral bands of ASTER in VNIR, SWIR and TIR parts of the electromagnetic spectrum and the possibility of applying several image processing algorithms (Pournamdary et al., 2014 a,b; Pour and Hashim, 2014). ASTER SWIR bands (six bands in the 1.6 to 2.43 µm wavelength region) contain sufficient spectral resolution to detect different spectral signatures for advanced argillic (alunite-kaolinite), sericitic (muscovite), propyllitic (epidote-chlorite-calcite) alteration mineral assemblages.

The main objective of this study is to test the most applicable image processing algorithms for detecting alteration

mineral assemblages in inaccessible regions without prior information or little available geological data of the study area (such Antarctic environments) using ASTER SWIR bands. In this research, the Oscar II coast area in north-eastern Graham Land, Antarctic Peninsula (AP) was selected to conduct a remote sensing satellite-based mapping approach. The image processing analysis was established based on target detection algorithms, including Constrained Energy Minimization (CEM), Orthogonal Subspace Projection (OSP) and Adaptive Coherence Estimator (ACE) to SWIR bands of ASTER for detecting spectral features of interest attributed to alteration mineral assemblages at district scale. To date, these algorithms are not yet tested and comparatively investigated for alteration mineral mapping applications in inaccessible regions, where prior geological data is little or not available.

2. MATERIALS AND METHODS

2.1 Geology of the study area

The Oscar II coast area is located in the north-eastern Graham Land, Antarctic Peninsula (AP) (Fig. 1). The lithological units in this area consisting of (i) volcanic and volcaniclastic rocks (Mapple Formation): a thick succession of Middle Jurassic, silicic, volcanic and volcaniclastic rocks, which is dominated by rhyolitic ignimibrite flows; (ii) intrusive rocks: acidic to intermediate plutons of various ages that include lithologies such as granite, granodiorite and diorite/gabbro; (iii) sedimentary rocks (Botany Bay and Trinity Peninsula Groups): these rocks conformably overlie up to 600 m thickness of terrestrial silt and mudstones that are attributed to the Lower to Middle Jurassic Botany Bay Group (BBG) and the Jurassic volcanic and sedimentary sequences rest unconformably upon heavily deformed Permian/Triassic quartzose meta-sedimentary rocks of the Trinity Peninsula Group (TPG). Lithological units of exposed rocks in the Oscar II coast area in the north-eastern Graham Land were mapped using ASTER data and laboratory spectral reflectance measurements of rock samples from the study areas by the British Antarctic Survey (BAS) (Haselwimmer et al., 2011).

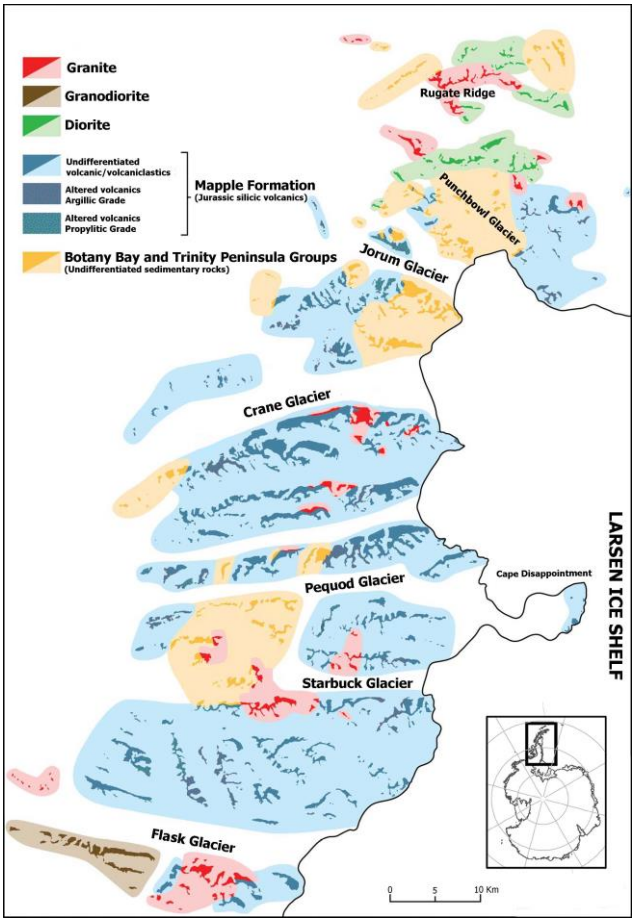

Figure 1. Geological map of the Oscar II Coast area (Haselwimmer et al. 2011).

2.2 Remote sensing data

The ASTER data used in this investigation were obtained from U.S. Geological EROS (http://glovis.usgs.gov/). Three ASTER level 1 T (Precision Terrain Corrected Registered At-Sensor Radiance) scenes covering the Oscar II coast region and surrounding areas (AST_L1T_00311222001131924, northern sector; AST_L1T_00311222001131933, central sector; AST_L1T_00311222001131942, southern sector) (Path/Row 218/106), north eastern part of Graham Land, Antarctic Peninsula (AP) were acquired on November 22, 2001. The ASTER Level 1 Precision Terrain Corrected Registered At Sensor Radiance (AST_L1T) data contains calibrated at sensor radiance, which corresponds with the ASTER Level 1B (AST_L1B), that has been geometrically corrected, and rotated to a north up UTM projection (https://lpdaac.usgs.gov/dataset_discovery/aster/aster_products_table/ast_l1t). The average of cloud cover for the ASTER data used in this study is less than 10 %. The images were pre-georeferenced to UTM zone 20 South projection using the WGS-84 datum. Figure 3 shows ASTER mosaicked color combination of bands 4, 6 and 8 as RGB for the Oscar II coast region and surrounding areas, north eastern part of Graham Land. In this study, the satellite remote sensing datasets were processed using the ENVI (Environment for Visualizing Images) version 5.2 and Arc GIS version 10.3 software packages.

2.3 Data analysis

Atmospheric correction serves a critical role in the processing of remotely sensed image data, particularly with respect to identification of pixel content. ASTER data (shortwave infrared bands) were converted to surface reflectance using Fast Line-of-sight Atmospheric Analysis of Spectral Hypercube (FLAASH) algorithm (Cooley et al., 2002). We applied the FLAASH algorithm with the Sub-Arctic Summer (SAS) atmospheric model and the Maritime aerosol model. Crosstalk correction was performed on the ASTER data sets used in this study (Iwasaki and Tonooka, 2005). Constrained Energy Minimization (CEM), Orthogonal Subspace Projection (OSP) and Adaptive Coherence Estimator (ACE) algorithms were selected for detecting alteration mineral assemblages using SWIR bands of ASTER data at district scale. These algorithms are not yet tested and comparatively investigated for alteration mineral mapping applications in inaccessible regions and polar context, where prior geological data is little or not available. Target detection algorithms were implemented to map fractional abundance of alteration mineral assemblages in some selected spatial subset scenes of the study region. Target detection algorithms carry out a partial unmixing method to isolate spectral feature of interest from the background and their output is a single score (abundance of the target) per pixel (Camps-Valls et al., 2012).

3. RESULTS AND DISCUSSION

CEM, OSP and ACE algorithms were applied to four selected spatial subset scenes of the study area. These districts were: (i) the zone between Crane Glacier and Pequod Glacier (Oscar II coast; mapped zone (see Fig. 1) and (ii) a section along the Rugate Ridge and Punchbowl Glacier (north Oscar II coast; poorly mapped zone (see Fig. 1). Figure 2 (A) shows the resultant image map derived from CEM algorithm for the zone between Crane Glacier and Pequod Glacier (Oscar II coast region). The distribution of sub-pixel abundance of alteration minerals agrees very well with the alteration zone classes extracted by Haselwimmer et al. (2011). However, the CEM algorithm was capable to detect detailed surface distribution of fractional abundance of alteration target minerals in the selected zone. In fact, previous alteration classes that simply assigned to chlorite-muscovite, muscovite-chlorite and muscovite contain variety of mineral assemblages (see zoom parts in Figure 2 (A)). Montmorillonite is one the high abundance alteration mineral in muscovite-chlorite class especially associated with exposed rocks near Crane Glacier. Biotite was detected in this study; previously it has been classified in many zones as low albedo area. In addition, detailed distribution of kaolinite and epidote in the study zone was mapped (see zoom parts in Figure 2 (A)).

Figure 2 (B) displays RGB image OSP map of kaolinite rule image (red), montmorillonite rule image (green) and chlorite (blue). Variety of colors is manifested in the pixel background of exposed lithology, including magenta, purple, pink, red, green, blue, yellow, cyan and white. The detected pixel classes are consistent with CEM resultant map (Fig. 2 (A)). High sub-pixel abundance value for kaolinite is coded in red (Fig. 2 (B)); therefore, zones contain high surface distribution of kaolinite appear in shades of red. Montmorillonite high abundance zones depict in shades of green in the rock exposure background. Blue color shade zones contain high sub-pixel abundance value of chlorite (Fig. 2 (B)). It is evident that in RGB image map the mixture pixel colors such as magenta, purple, pink, yellow, cyan and white represent combination of alteration mineral assemblages. For instance, yellow color represents a mixture of kaolinite and montmorillonite; purple color exhibits a mixture of kaolinite and chlorite; magenta, cyan, pink and white colors characterize different combinations of sub-pixel abundance of kaolinite, montmorillonite and chlorite mineral assemblages (Fig. 2 (B)).

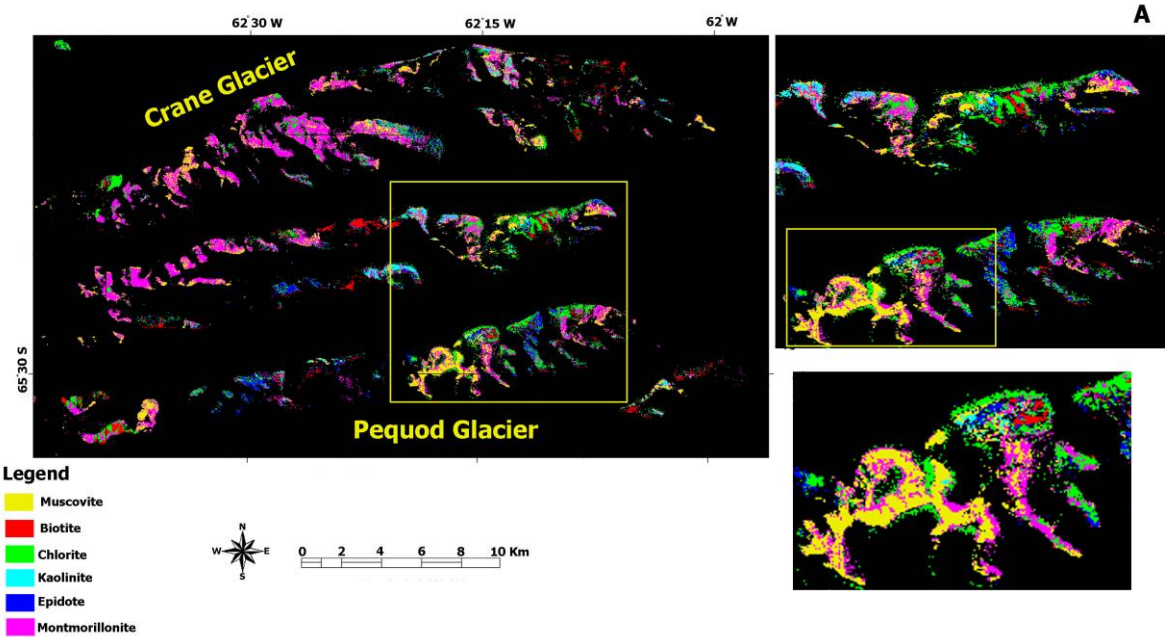

Figure 2. (A) Resultant image map derived from CEM algorithm for the zone between Crane Glacier and Pequod Glacier (Oscar II coast region).

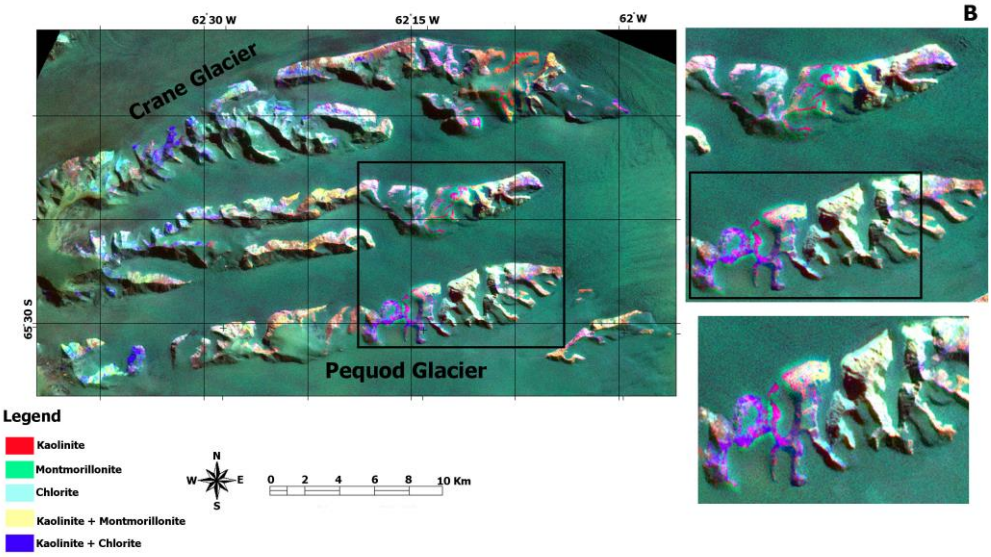

Figure 2. (B) Resultant image map derived from OSP algorithm for the zone between Crane Glacier and Pequod Glacier (Oscar II coast region).

ACE algorithm was also implemented to the selected spatial subset zone (between Crane Glacier and Pequod Glacier; Oscar II coast region) of the study area. Resultant gray scale (rule) images depict high DN values of the sub-pixel abundance of the target mineral in the study zone. Rule image classifier tool was used to produce a classified image map. But, the image map contains very noisy background, and classified mineral zones were not discernable from the background.

Fractional abundance of alteration target minerals in the CEM resultant map for the section along the Rugate Ridge and Punchbowl Glacier, Oscar II coast area is shown in Figure 3 (A). Chlorite, biotite, muscovite, kaolinite and epidote are dominated alteration minerals in this zone, respectively. With reference to geology (Fig. 1) and alteration mineral maps of the Oscar II coast area, chlorite abundance zones (green pixels) are associated with propylitically-altered volcanic rocks. Biotite high abundance zones (red pixels) are coincided with dioritic exposures. Association of muscovite (yellow pixels) and kaolinite (cyan pixels) are matched with sericitically-argillically altered volcanic rocks (see zoom parts in Figure 3 (A)). Granitic exposures in Rugate Ridge are governed by kaolinite abundance zones. However, combination of chlorite, biotite, muscovite, kaolinite and epidote mineral assemblages are mapped in the zone of undifferentiated sedimentary rocks (Botany Bay and Trinity Peninsula groups). Concerning

previous investigation and existing ground truth information (Haselwimmer et al., 2011) in the section along the Rugate Ridge and Punchbowl Glacier, several unassigned (insufficient mapped pixels) and low albedo zones were identified and classified using CEM algorithm as high surface distribution of alteration minerals especially biotite, kaolinite and epidote in this zone.

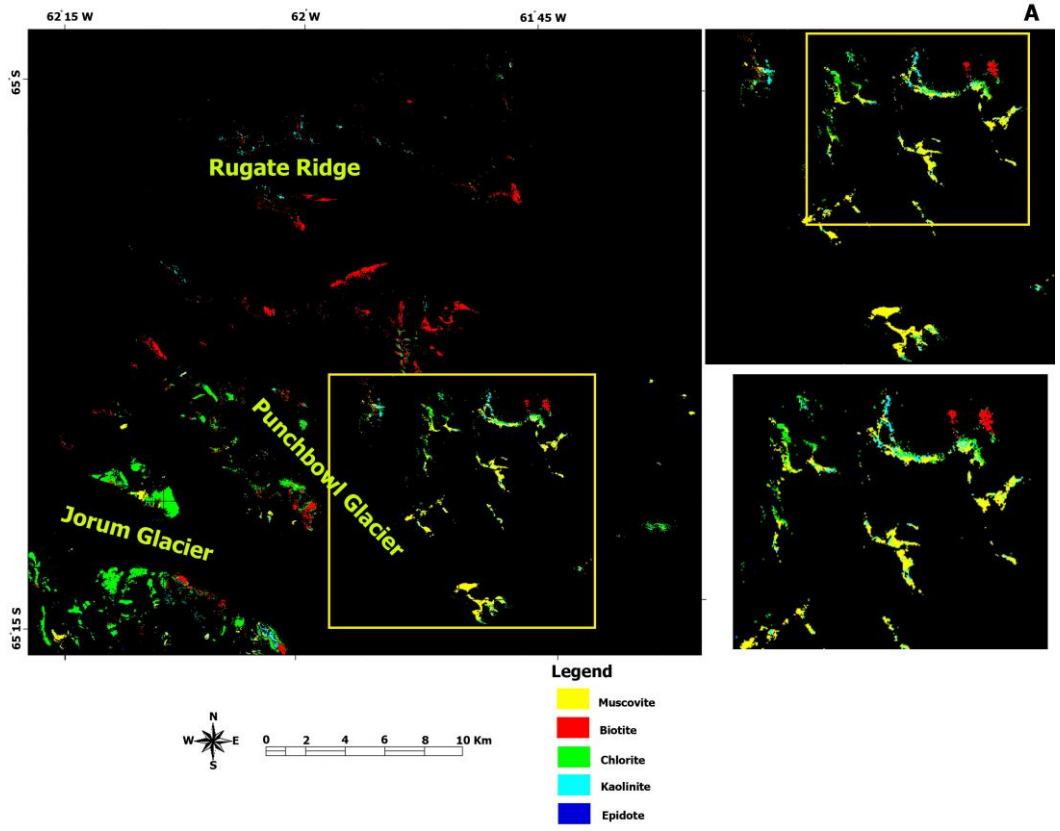

Figure 3. (A) Resultant image map derived from CEM algorithm for the section along the Rugate Ridge and Punchbowl Glacier (Oscar II coast region).

Figure 3 (B) shows OSP FCC image map for the study zone along the Rugate Ridge and Punchbowl Glacier, which is produced by assigning muscovite rule image to red color, chlorite to green color and biotite to blue, respectively. High abundance muscovite zones (shades of red) are appeared in the south-eastern sector of the study zone (see zoom parts in Figure 3 (B)), which are consistent with alteration mineral map (see Fig. 1) and CEM resultant map (Fig. 3 A). Chlorite (shades of green) and biotite (shades of blue) are agreed well with the reference data. However, some zones contain high abundance of biotite (according to CEM rule image) are appeared as bright pixels in the background of exposed lithologies. It might be due to combination of biotite with other alteration minerals.

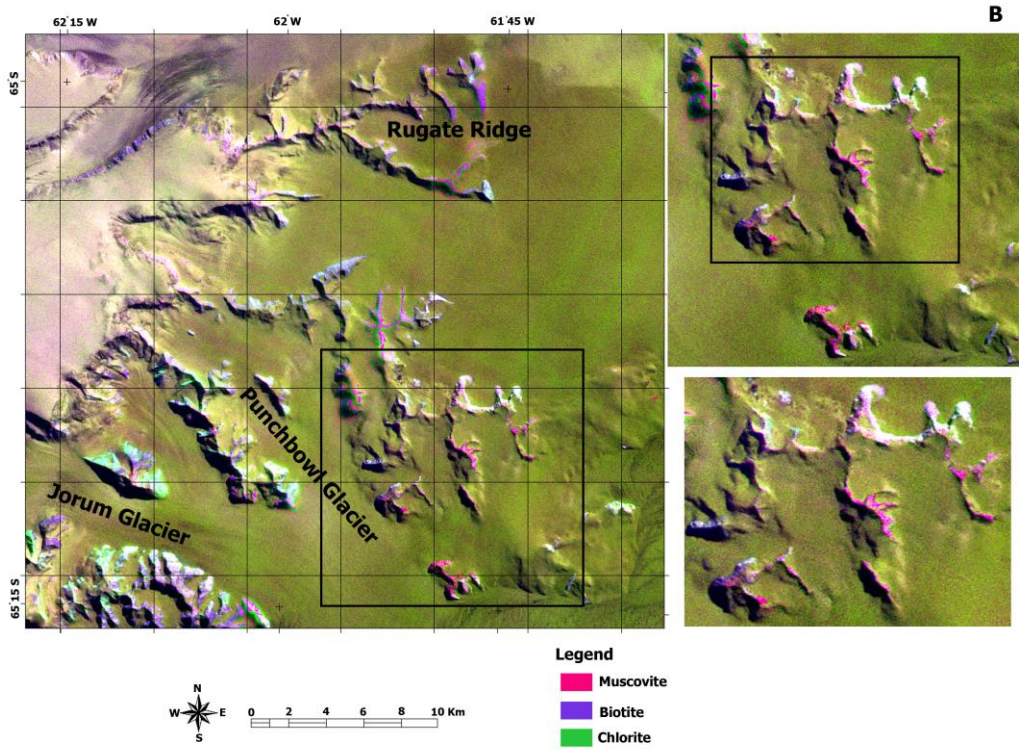

Figure 3. (B) Resultant image map derived from OSP algorithm for the section along the Rugate Ridge and Punchbowl Glacier (Oscar II coast region).

4. CONCLUSIONS

The remote sensing satellite-based approach used in this investigation to map poorly exposed lithologies has been shown to perform extremely well in the inaccessible regions (Antarctic environments). It could be comprehensively used for alteration mapping and hydrothermal ore mineral exploration in other inaccessible regions. This investigation has indicated the application of SWIR bands of ASTER datasets for extrapolating satellite-based imagery from relatively mapped area such Oscar II coast area, in north-eastern Graham Land, Antarctic Peninsula (AP) into poorly mapped or unmapped (further north and south) domains. Image processing algorithms mapped sub-pixel abundance distribution of Al-O-H, Fe, Mg-O-H and CO3 mineral groups. The capability to distinguish fractional abundance of alteration minerals using CEM, OSP and ACE algorithms provided invaluable information for discrimination lithological units and alteration mineral assemblages in remote and inaccessible terrains at district scale. Sub-pixel abundance value of mafic minerals such as epidote, chlorite and biotite (Fe, Mg-OH absorption), K-feldspar alteration products (kaolinite, illite, montmorillonite) and muscovite (Al-OH absorption) was detected using ASTER SWIR bands in poorly mapped and unmapped regions in the northern and southern sectors of Oscar II coast area, Graham Land. The approach used in this study performed very well for lithological and alteration mineral mapping with little available geological data or without prior information of the study region.

ACKNOWDEGMENT
This study was supported by KOPRI grant PE17050 for Post-Doctoral researcher. We are thankful to Korea Polar Research Institute (KOPRI) for providing all the facilities for this investigation.

REFERENCES

Abrams, M., Hook, S. and Ramachandran, B., 2004. ASTER User Handbook, Version *2*. Jet Propulsion Laboratory, California Institute of Technology. Online: http://asterweb.jpl. nasa.gov/content/03_data/04_Documents/aster_ guide_ v2.pdf.

Camps-Valls, G., Tuia, D., Gómez-Chova, L., Jiménez, S., Malo, J., 2012. Remote Sensing Image Processing. Morgan & Claypool Publishers.

Cooley, T., Anderson, G.P., Felde, G.W., Hoke, M.L., Ratkowski, A.J., Chetwynd, J.H., Gardner, J.A., Adler-Golden, S.M., Matthew, M.W., Berk, A., Bernstein, L.S., Acharya, P.K., Miller, D., Lewis, P., 2002. FLAASH, a MODTRAN4-based atmospheric correction algorithm, its application and validation. Proceedings of the Geoscience and Remote Sensing Symposium, 2002, IEEE International, 3, 1414–1418.

Haselwimmer, C. E., Riley, T. R. and Liu J. G. 2011. Lithologic mapping in the Oscar II Coast area, Graham Land, Antarctic Peninsula using ASTER data. International Journal of Remote Sensing, 32(7), 2013-2035.

Iwasaki, A., Tonooka, H., 2005. Validation of a crosstalk correction algorithm for ASTER/SWIR. IEEE Transactions of Geoscience and Remote Sensing 43(12), 2747-2751.

Pour, B. A., Hashim, M., 2014. ASTER, ALI and Hyperion sensors data for lithological mapping and ore mineral exploration. Springerplus, 3(130), 1-19.

Pour, A.B., Hashim, M., Park, Y., Hong, J.K. 2017a. Mapping alteration mineral zones and lithological units in Antarctic regions using spectral bands of ASTER remote sensing data. Geocarto International, doi.org/10.1080/10106049.2017.1347207.

Pour, A.B., Hashim, M., Hong, J.K., Park, Y. 2017b. Lithological and alteration mineral mapping in poorly exposed lithologies using Landsat-8 and ASTER satellite data: north-eastern Graham Land, Antarctic Peninsula. Ore Geology Reviews, doi.org/10.1016/j.oregeorev.2017.07.018

Pournamdary M, Hashim M, Pour BA. 2014a. Application of ASTER and Landsat TM data for geological mapping of Esfandagheh ophiolite complex, southern Iran. Resource Geology 64 (3), 233-246.

Pournamdary M, Hashim M. Pour BA. 2014b. Spectral transformation of ASTER and Landsat TM bands for lithological mapping of Soghan ophiolite complex, south Iran. Advances in Space Research 54 (4), 694-709.